MOLECULAR AND CELLULAR BIOLOGY, Sept. 2001, p. 6189–6197 Vol. 21, No. 18
0270-7306/01/$04.00+0 DOI: 10.1128/MCB.21.18.6189–6197.2001

Functional Analysis of Asb-1 Using Genetic Modification in Mice

BENJAMIN T. KILE,* DONALD METCALF, SANDRA MIFSUD, LADINA DIRAGO, NICOS A. NICOLA, DOUGLAS J. HILTON, AND WARREN S. ALEXANDER

The Walter and Eliza Hall Institute of Medical Research and The Cooperative Research Centre for Cellular Growth Factors, Royal Melbourne Hospital, Victoria 3050, Australia

Received 30 March 2001/Returned for modification 8 June 2001/Accepted 11 June 2001

The Asbs are a family of ankyrin repeat proteins that, along with four other protein families, contain a C-terminal SOCS box motif, which was first identified in the suppressor of cytokine signaling (SOCS) proteins. While it is clear that the SOCS proteins are involved in the negative regulation of cytokine signaling, the biological roles of the other SOCS box-containing families are unknown. We have investigated Asb-1 function by generating mice that lack this protein, as well as mice that overexpress full-length or truncated Asb-1 in a wide range of tissues. Although Asb-1 is expressed in multiple organs, including the hematopoietic compartment in wild-type mice, Asb-1$^{-/-}$ mice develop normally and exhibit no anomalies of mature blood cells or their progenitors. While most organs in these mice appear normal, the testes of Asb-1$^{-/-}$ mice display a diminution of spermatogenesis with less complete filling of seminiferous tubules. In contrast, the widespread overexpression of Asb-1 in the mouse has no apparent deleterious effects.

The suppressor of cytokine signaling (SOCS) box is an approximately 40-amino-acid motif found in five distinct families of proteins (7). It was first identified in the SOCS family of negative regulators of cytokine signaling, which comprise amino-terminal regions of variable amino acid sequence and length and a central SH2 domain, in addition to the carboxy-terminal SOCS box (21). SOCS proteins block the JAK/STAT signaling pathway and can thus inhibit signaling initiated by a diverse array of cytokines, hormones, and growth factors (9). The physiological roles of the SOCS proteins are beginning to be elucidated by gene inactivation studies in mice. A key role for SOCS1 in gamma interferon signaling was identified in SOCS1$^{-/-}$ mice, which die before weaning from a complex gamma interferon-dependent disease characterized by fatty degeneration of the liver, lymphopenia, and monocytic infiltration of multiple organs (3, 13, 20). Essential roles for SOCS2 in the regulation of postnatal growth hormone–IGF-1 signaling (14) and for SOCS3 in the regulation of fetal erythropoiesis (12) have also been postulated from the phenotypes of their respective knockout mice.

Several studies suggest that the SOCS box functions as an adaptor, recruiting SOCS box-containing proteins and their interacting partners to a core ubiquitination complex via interaction with elongins B and C (8, 23). Whether this mechanism is used to regulate SOCS protein levels, partner protein levels, or both is unclear, and the interaction between the SOCS box and elongins B and C remains to be demonstrated in vivo. The four other protein families that possess a SOCS box differ from the SOCS proteins in the domains upstream of this motif and have been categorized accordingly: rather than SH2 domains, the WSBs contain WD-40 repeats, the SSBs contain SPRY domains, the RAR-like proteins contain GTPase domains, and the ASBs contain ankyrin repeats (7). In contrast to the SOCS proteins, nothing is known of either the functions of the more than 20 members of these latter four families or whether they play a role in the negative regulation of cytokine signaling. We have recently cloned four members of the Asb family (10), and we present here data from mice with inactivation of the Asb-1 gene, as well as transgenic mice ubiquitously overexpressing this protein. The data suggest that deletion or overexpression of Asb-1 has no obvious deleterious effects on normal mouse development and hemopoiesis but that an increased frequency of testicular anomalies accompanies the loss of Asb-1.

* Corresponding author. Mailing address: The Walter and Eliza Hall Institute for Medical Research, Post Office, Royal Melbourne Hospital, Victoria 3050, Australia. Phone: 61-3-9345-2653. Fax: 61-3-9345-2616. E-mail: kile@wehi.edu.au.

MATERIALS AND METHODS

All restriction enzymes were obtained from Roche (Mannheim, Germany). Oligonucleotides were manufactured by Genset Pacific (Lismore, Australia) and Geneworks (Adelaide, Australia).

Generation of targeted ES cells and Asb-1$^{-/-}$ mice. A fragment of the murine Asb-1 gene extending ~3.2 kbp 5′ from the beginning of exon 2 was generated by PCR using oligonucleotides containing *Bam*HI (5′; primer; 5′-AGCTGGATCCCGTCCGGGACTCGGGTCC-3′) and *Bgl*II (3′ primer; 5′-AGCTAGATCTGCCATAGGACCTGCACTGAAGAG-3′) restriction sites. This fragment was digested with *Bam*HI, and the resultant 0.9-kb 3′ fragment was ligated directly upstream of the initiation codon of β-galactosidase via a *Bam*HI site in the plasmid pβgalGFPpAloxneo, which also contains a PGKneo cassette flanked by *loxP* sites (20). Subsequently, the vector was digested with *Bam*HI and the larger 2.3-kb *Bam*HI fragment of the initial 5′-arm PCR product was ligated directly upstream of the smaller fragment, generating a 3.2-kb 5′ arm. A 4.3-kb *Bam*HI fragment from the genomic Asb-1 locus was cloned into the *Bam*HI site of the plasmid pBS-2*Xho* and then excised with *Xho*I and cloned into a *Xho*I site 3′ to the PGKneo cassette. This construct was linearized and electroporated into C57BL/6-derived embryonic stem (ES) cells. Clones surviving selection in 175 μg of G418/ml were screened for those in which the targeting construct had recombined with an endogenous Asb-1 allele by probing Southern blots of *Eco*RI-digested genomic DNA with a 1.5-kb PCR fragment lying upstream of exon 1 as described previously (1). A targeted ES cell clone was injected into BALB/c blastocysts to generate chimeric mice. Male chimeras were mated with C57BL/6 females to yield Asb-1 heterozygotes which were interbred to produce wild-type (Asb-1$^{+/+}$) and heterozygous (Asb-1$^{+/-}$) and homozygous (Asb-1$^{-/-}$) mutant mice. The genotypes of offspring were determined by Southern blot analysis of genomic DNA extracted from tail biopsy specimens as described above. The deletion of Asb-1 exon 3 and the inability of Asb-1$^{-/-}$ mice to produce Asb-1 mRNA were confirmed in nucleic acid blots performed as described previously (10). Southern blots of restriction enzyme-digested genomic DNA were probed

with a 300-bp fragment of Asb-1 exon 3 sequence (A1-e3). Northern blots were probed with a 1.0-kb fragment of Asb-1 cDNA comprising the entire coding sequence, before being stripped and reprobed with a 1.2-kb *Pst*I fragment of glyceraldehyde-3-phosphate dehydrogenase cDNA (GAPDH) as described previously (1).

Generation of Asb-1 transgenic mice. The UBI-*junB* plasmid (18), which contains a 1,225-bp fragment of the human ubiquitin C promoter, was modifed to remove the *junB* cDNA and add a Kozak sequence, an ATG initiation codon, an *Asc*I site, and a FLAG epitope sequence to generate the plasmid pUbiFLAG. A fragment of the murine Asb-1 cDNA comprising the entire 1,005-bp coding region was generated by PCR using oligonucleotides containing *Asc*I (5′ primer; 5′-AGCTGGCGCGCCAGGCGGAGGGCGGGACCGGCCCC-3′) and *Mlu*I (3′ primer; 5′-AGCTACGCGTCTCATAAAGCAAAAACTTCTT-3′) restriction sites. This fragment was digested with *Asc*I and *Mlu*I and ligated directly into the *Asc*I site of pUbiFLAG, which also contains a poly(A) and simian virus 40 intron and splice junction. A similar construct was generated utilizing an 879-bp fragment of the murine Asb-1 cDNA comprising the entire coding region minus the SOCS box sequence (3′ primer; 5′-AGCTACGCGTCTTCTGGCCTCTTT AAAGACCTGCAAGGC-3′). Both constructs were linearized, agarose gel purified, and injected into the male pronucleus of C57BL/6 fertilized eggs, which were transferred to pseudopregnant females. Offspring were tested for the integration of the transgene by Southern blot hybridization of total genomic DNA digested with *Xba*I and probed with A1-e3. Colonies of mice were established from two founders positive for each transgene. Expression of the transgene was confirmed at the mRNA level by Northern blot hybridizations utilizing probe A1-e3, before the blots were stripped and reprobed with the 1.2-kb fragment of GAPDH cDNA.

Analysis of protein expression in Asb-1 transgenic mice. Tissues were removed from Asb-1 transgenic mice and wild-type littermates and frozen in liquid nitrogen. They were then pulverized and Dounce homogenized on ice in 1 to 2 ml per organ of KALB lysis buffer (16) containing protease inhibitors (Complete Cocktail tablets; Roche). Immunoprecipitations were performed on lysates containing 5 to 20 mg of protein using M2 anti-FLAG affinity resin (Sigma Chemical Co., St. Louis, Mo.) and separated by sodium dodecyl sulfate-polyacrylamide gel electrophoresis (Bio-Rad Laboratories, Hercules, Calif.). Protein was then electrophoretically transferred to PVDF-Plus membranes (Micron Separations Inc., Westborough, Mass.). Membranes were blocked overnight in 10% skim milk and incubated with rat anti-FLAG antibody for 2 h. Antibody binding was visualized with peroxidase-conjugated goat anti-rat immunoglobulin (Southern Biotechnology, Birmingham, Ala.) and the enhanced chemiluminescence (ECL) system (Amersham Pharmacia, Little Chalfont, United Kingdom). To control for loading, lysate volumes containing 50 to 200 μg protein were separated by sodium dodecyl sulfate-polyacrylamide gel electrophoresis, transferred to PVDF-Plus, and blocked overnight before being incubated with rat anti-HSP70 antibody.

Histopathological analysis. Tissues (uterus, bladder, liver, testes, seminal vesicle, skin, eye, kidney, heart, lung, thymus, salivary gland, small intestine, muscle, brain, spleen, and pancreas) were weighed (with the exception of skin and eyes), fixed in 10% buffered formalin, and embedded in paraffin, and sections were prepared by standard techniques, stained with hematoxylin and eosin, and examined by light microscopy. The peripheral blood white cell and platelet counts were determined manually using hemocytometers. Single-cell suspensions from femoral bone marrow, spleen, liver, and peritoneum were prepared by standard techniques, and differential cell counts were performed on smears or cytocentrifuge preparations stained with May-Grunwald-Giemsa stain.

β-Galactosidase histochemistry. Mice were killed by cervical dislocation, and tissues were removed immediately and fixed in 4% paraformaldehyde–mouse tonicity phosphate-buffered saline (MT PBS) at 4°C for 1 h. After being washed in MT PBS three times for 30 min each at room temperature, tissues were incubated overnight at 37°C in staining solution (100 mM sodium phosphate [pH 7.3], 2 mM $MgCl_2$. 0.01% sodium deoxycholate, 0.02% Nonidet P-40, 5 mM potassium ferricyanide, 5 mM potassium ferrocyanide, 1 mg of X-Gal [5-bromo-4-chloro-3-indolyl-β-D-galactopyranoside] per ml). Tissues were washed in MT PBS three times for 30 min each and postfixed overnight in 4% paraformaldehyde–MT PBS at 4°C, before sections were prepared, stained with nuclear fast red, and examined by light microscopy.

Flow cytometry. Dispersed cell suspensions from bone marrow, spleen, thymus, and mesenteric lymph node from 8-week-old Asb-$1^{-/-}$ mice and wild-type littermates were prepared, and the erythrocytes were lysed as described previously (5). The cells were stained with rat monoclonal antibodies for specific cell surface markers and analyzed by flow cytometry as described previously (22). Transcription of the β-galactosidase gene under the control of the Asb-1 promoter in the Asb-$1^{-/-}$ mice was monitored by detecting β-galactosidase activity (fluorescence-activated cell sorting [FACS]–Gal analysis) as described previously (5).

Agar cultures. Semisolid 1-ml agar cultures containing 2.5×10^4 bone marrow cells or 5×10^4 spleen cells were prepared using Dulbecco modified Eagle medium containing a final concentration of 20% newborn calf serum and 0.3% agar, in 35-mm plastic petri dishes. Colony formation was stimulated in replicate cultures by addition of serial dilutions of 0.1 ml of recombinant granulocyte-macrophage colony stimulating factor (GM-CSF), macrophage CSF (M-CSF), granulocyte CSF (G-CSF), interleukin 3 (IL-3), or stem cell factor (SCF). Cultures were incubated for 7 days in a fully humidified atmosphere of 10% CO_2 in air. After initial scoring at ×35 magnification, cultures were fixed by the addition of 1 ml of 2.5% glutaraldehyde. Four hours later, the cultures were floated intact onto glass slides and, after drying, were stained in sequence for acetylcholinesterase and then with Luxol Fast Blue (BDH Laboratory, Poole, United Kingdom) and hematoxylin. After mounting under coverslips, the cultures were analyzed at ×200 and ×100 magnifications to determine the number and composition of colonies in the entire cultures.

CFU-spleen (CFU-S) studies. Bone marrow cells from five Asb-$1^{-/-}$ and five wild-type C57BL/6 control mice were injected into irradiated wild-type C57BL/6 mice as described previously (11). Spleens were removed after 8 days and fixed in Carnoy's solution, and the numbers of macroscopic colonies were counted.

Phenylhydrazine challenge. Female Asb-$1^{-/-}$ and wild-type C57BL/6 control mice received two intraperitoneal injections of freshly prepared phenylhydrazine in mouse tonicity RPMI medium (totalling ~25 μg/kg of body weight) on day 0. Three mice of each genotype were bled and sacrificed on days 0, 4, and 12. Blood was analyzed using an Advia120 automated hematological analyzer (Bayer, Leverkusen, Germany). Spleen and bone marrow cells were cultured in 1.5% methylcellulose as described previously (2) in the presence of SCF, IL-3, and erythropoietin (EPO), or EPO alone. Numbers of CFU-EPO (CFU-E) and burst-forming unit–EPO (BFU-E) were scored after 2 and 7 days, respectively.

Endotoxin. Endotoxin (lipopolysaccharide [LPS]; Difco, Detroit, Mich.) was dissolved in 0.9% sodium chloride solution, and 5 μg was injected intravenously in an injection volume of 0.2 ml into 12 Asb-$1^{-/-}$ and 12 wild-type mice. Six days after injection, mice were anesthetized using penthrane and bled from the axilla. Single-cell suspensions were prepared from bone marrow and spleen. Differential counts were performed, and spleen cells were cultured in semisolid agar in the presence of GM-CSF, IL-3, or M-CSF.

Local peritoneal cavity inflammation and infection. Mice were injected interperitoneally with 2 ml of an 0.2% (wt/vol) solution of casein C5890 (Sigma) in MT PBS. The Sigma preparation is contaminated by viable saprophytic *Bacillus* organisms (15). Three hours after injection, the mice were killed by anesthesia, the abdominal cavity was injected with 2 ml of MT PBS, and after massage to mix peritoneal cells with injected harvesting fluid, the cell suspension was removed using a soft plastic pipette. Absolute and differential counts were performed on harvested peritoneal cells, and dispersed cell suspensions were prepared from the spleen and bone marrow.

Serum biochemistry. Six 3-month-old Asb-$1^{-/-}$, Asb-1 transgenic, and C57BL/6 control animals were anesthetized using penthrane and bled from the axilla. Biochemical analyses were performed by the IDEXX Central Veterinary Diagnostic Laboratory (Melbourne, Australia).

RESULTS

Generation of Asb-$1^{-/-}$ mice. To investigate the in vivo function of Asb-1, we used gene targeting to generate Asb-$1^{-/-}$ mice. The vector was designed not only to eliminate *asb-1* function but also to place a β-galactosidase gene under the control of the endogenous *asb-1* promoter (see Materials and Methods) (Fig. 1a). After electroporation of the construct into ES cells, a clone in which homologous recombination had occurred was injected into blastocysts to generate chimeric mice and subsequently Asb-$1^{+/-}$ mice. Southern blot hybridization analysis at weaning (Fig. 1b) revealed that offspring of heterozygous parents included mice of the expected three genotypes in approximately Mendelian proportions (20:37:16 for Asb-$1^{+/+}$, Asb-$1^{+/-}$, and Asb-$1^{-/-}$, respectively). Southern analysis also confirmed the deletion of exon 3 as predicted by the targeting strategy (Fig. 1c). Northern blot hybridization analysis of RNA extracted from a range of organs established

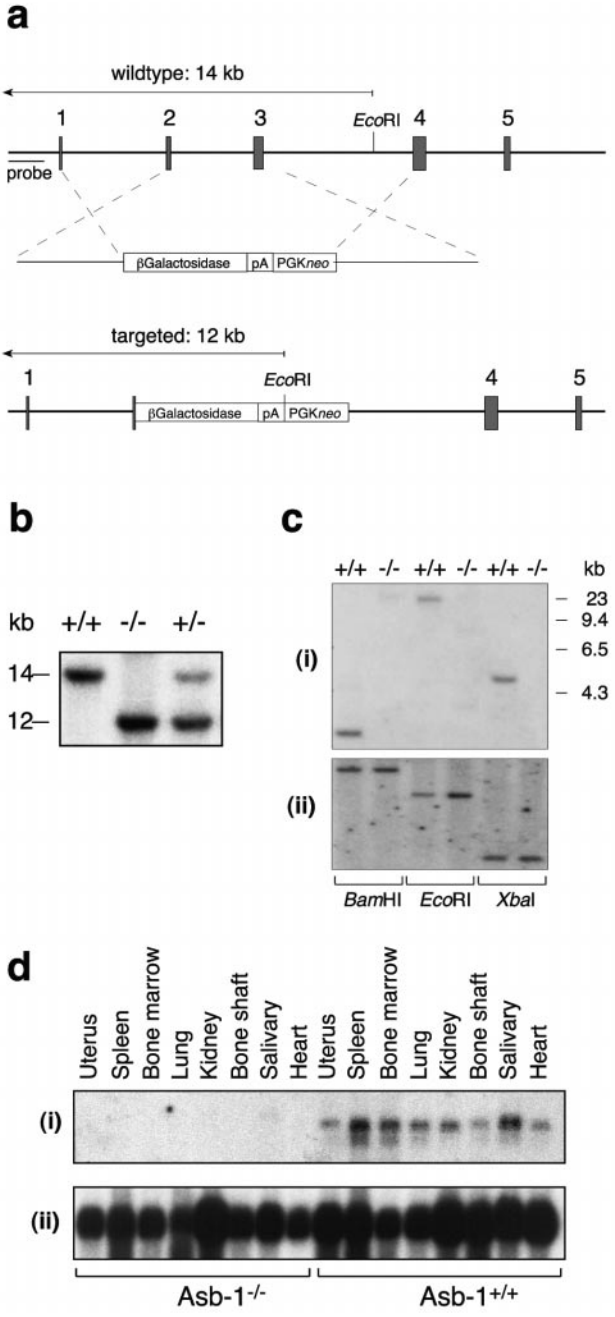

FIG. 1. Disruption of the Asb-1 locus by homologous recombination. (a) The functional murine Asb-1 gene, with the exons containing coding regions shown as shaded boxes. In the targeted allele, exon 3 and the majority of exon 2 were replaced by a βGalPGKneo cassette, in which the β-galactosidase coding region was fused in-frame to the third codon of exon 2. (b) Southern blot of *Eco*RI-digested genomic DNA from the tails of mice derived from a cross between Asb-$1^{+/-}$ mice. The blot was hybridized with the 5′ genomic Asb-1 probe, which distinguishes between endogenous (14-kb) and targeted (12-kb) alleles. (c) Southern blot of genomic DNA from the tails of Asb-$1^{-/-}$ mice and wild-type littermates. (i) Blot hybridized with a 300-bp exon 3 probe, confirming the deletion of exon 3. (ii) As a loading control, the blot was stripped and reprobed with a 200-bp probe corresponding to the SOCS box region of the *asb-1* gene. (d) Northern blot showing lack of Asb-1 expression in organs of Asb-$1^{-/-}$ mice. (i) The blot was hybridized with a coding region probe, which detects the 5.5-kb transcript; (ii) the integrity of the RNA was confirmed by hybridization with GAPDH.

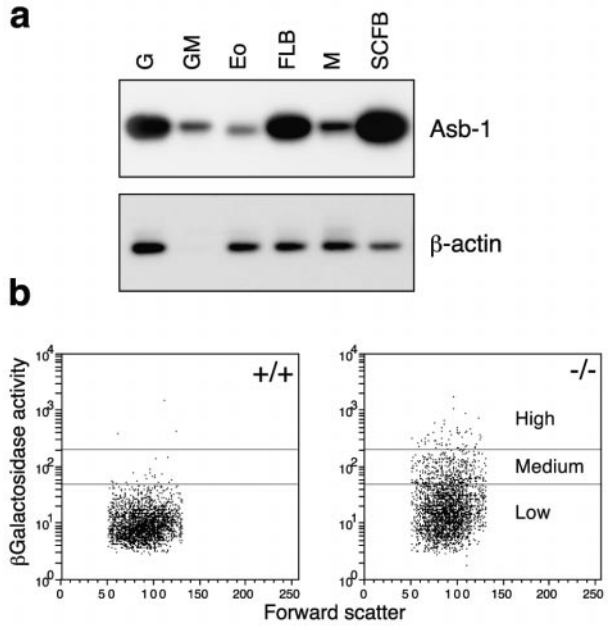

FIG. 2. Expression of Asb-1 in hematopoietic cells. (a) Reverse transcription-PCR performed on RNA isolated from mature colonies of granulocytes (G), granulocytes-macrophages (GM), cosinophils (Eo), flk ligand-stimulated blast cells (FLB), macrophages (M), and SCF-stimulated blast cells (SCFB). (b) Fluorescence-activated sorting of bone marrow cells from adult Asb-$1^{+/+}$ and Asb-$1^{-/-}$ mice according to β-galactosidase activity. Asb-$1^{-/-}$ bone marrow was sorted into three fractions designated βGal^{High}, βGal^{Medium}, and βGal^{Low}, which represented 10, 20, and 70% of the total population, respectively.

that Asb-1 transcripts were undetectable in homozygous mutant mice (Fig. 1d), confirming that the Asb-1 gene had been functionally deleted. Asb-$1^{+/-}$ and Asb-$1^{-/-}$ mice both developed normally, with males and females being fertile. In addition, the mutant mice showed no obvious external defects and lived in apparent good health for at least 12 months. The weights of 15 organs from each of six male and six female

TABLE 1. Percent distribution of β-galactosidase-positive progenitor cells in the bone marrow of Asb-$1^{-/-}$ mice

β-galactosidase activity	Stimulus	% Distribution[a]					
		Blast	G	GM	M	Eo	Meg
High	GM-CSF	20	62	43	57	100	
	IL-3	20	51	19	18	63	27
	SCF	25	34				
	SCF + IL-3 + Epo	20	51	11	43	66	29
Medium	GM-CSF		38	33	33	0	
	IL-3	63	41	45	59	37	73
	SCF	63	60				
	SCF + IL-3 + Epo	54	46	67	46	34	65
Low	GM-CSF		0	23	10	0	
	IL-3	17	8	36	23	0	0
	SCF	12	6				
	SCF + IL-3 + Epo	26	3	22	11	0	6

[a] Values shown are the percentages in each FACS Gal fraction of the absolute number of colonies of each lineage present in all three fractions. G, granulocytic; GM, granulocyte-macrophage; M, macrophage; Eo, eosinophil; Meg, megakaryocyte.

TABLE 2. Peripheral blood cell parameters for Asb-1$^{-/-}$ mice and wild-type littermates[a]

Parameter	Asb-1$^{-/-}$ (n = 6)	Asb-1$^{+/+}$ (n = 6)
Cells/μl (total)	3,120 ± 1,900	2,230 ± 1,220
Neutrophils	350 ± 340	280 ± 210
Lymphocytes	2,410 ± 1,190	1,810 ± 1,270
Monocytes	250 ± 370	110 ± 50
Eosinophils	120 ± 80	30 ± 30
Platelets/μl	908,950 ± 74,580	871,560 ± 137,770
Hematocrit (%)	47 ± 2	47 ± 2

[a] Values are means ± standard deviations.

Asb-1$^{-/-}$ mice were compared with those for six wild-type mice, and with the exception of the spleen (discussed below), no statistically significant differences were observed. Levels in serum of albumin, globulin, bilirubin, aspartate aminotransferase, alkaline phosphatase, urea, creatinine, sodium, potassium, chloride, calcium, and creatine kinase in Asb-1$^{-/-}$ mice were within the normal range observed in wild-type mice.

Expression of Asb-1 in hematopoietic cells. In the adult mouse, Asb-1 mRNA expression was detected in most organs, most prominently in spleen, bone marrow, and salivary gland (Fig. 1d). To determine whether expression in the bone marrow was restricted to any particular subset of hematopoietic cells, we conducted reverse transcription-PCR on mRNA isolated from colonies of various lineages (Fig. 2a). This analysis revealed that Asb-1 mRNA is expressed in mature granulocytes, macrophages, and eosinophils and also in the cells of blast colonies stimulated to develop by SCF or flk-2/flt-3 ligand and leukemia inhibitory factor. To refine this analysis, we stained Asb-1$^{-/-}$ bone marrow for β-galactosidase activity and, using gates set relative to the wild-type profile, sorted the Asb-1$^{-/-}$ population into three fractions designated βGal^{High}, βGal^{Medium}, and βGal^{Low}, which contained 10, 20, and 70% of the total cells, respectively (Fig. 2b). Culturing 10,000 cells from each fraction in the presence of GM-CSF, multi-CSF, or SCF revealed that, for all three stimuli, the majority of progenitor cells from all lineages were present in the βGal^{High} or βGal^{Medium} fractions, suggesting that most progenitor cells transcribe Asb-1 (Table 1). Furthermore, cytological analysis of βGal^{High} or βGal^{Medium} marrow populations showed the presence in each fraction of mature cells of all lineages, with some enrichment of blast cells. These data indicate that Asb-1 continues to be expressed in many hematopoietic cells until full maturation is attained.

Hematopoiesis in Asb-1$^{-/-}$ mice. Cell numbers and morphology were normal in the peripheral blood of Asb-1$^{-/-}$ mice (Table 2), and examination of stained cytocentrifuge preparations from bone marrow and spleen revealed no significant differences in the frequencies of hematopoietic subsets between adult Asb-1$^{-/-}$ mice and their wild-type littermates (data not shown). Although most progenitor cells express Asb-1, no difference was observed in the response of bone marrow or spleen progenitor cells stimulated to proliferate by GM-CSF, G-CSF, SCF, IL-3, or M-CSF (Table 3) or when stimulated by titrations of GM-CSF and IL-3. In each case the number, type, and size of colonies developing were similar in Asb-1$^{-/-}$ and Asb-1$^{+/+}$ mice. FACS analysis of adult bone marrow cells, splenocytes, thymoctes, and mesenteric lymph node cells incubated with antibodies to cell surface markers of the erythroid, myeloid, and lymphoid lineages (anti-Ter119, CD44, Mac-1, Gr-1, F4/80, B220, surface immunoglobulin, Mel-14, Thy-1, CD4, or CD8) also revealed no significant differences (data not shown). Cells in the hematopoietic stem cell compartment were examined by comparing the frequency of day 8 CFU-S in the bone marrow of Asb-1$^{-/-}$ mice with those of wild-type controls. Wild-type bone marrow cells yielded on average 8.6 ± 3.0 CFU-S_{d8} per 10^5 bone marrow cells, while Asb-1$^{-/-}$ marrow contained similar numbers, 9.7 ± 3.9 CFU-S_{d8} per 10^5 bone marrow cells.

Following an initial observation that the spleens of Asb-1$^{-/-}$ mice appeared to be smaller than those of wild-type litter-

TABLE 3. Culture of Asb-1$^{-/-}$ and C57BL/6 control bone marrow and spleen cells[a]

Cell no. and type	Stimulus	Mean no. of colonies					
		Blast	G	GM	M	Eo	Meg
2.5 × 10^4 bone marrow cells/culture							
Asb-1$^{-/-}$ (n = 4 to 6)	GM-CSF		12 ± 3	5 ± 1	27 ± 12	1 ± 1	
	G-CSF		10 ± 5	0	0		
	M-CSF		1 ± 1	4 ± 3	35 ± 7		
	IL-3	5 ± 3	17 ± 18	10 ± 2	18 ± 8	2 ± 1	3 ± 1
	SCF	4 ± 2	16 ± 5	1 ± 1	0		
C57BL/6 (n = 4 to 6)	GM-CSF		12 ± 4	6 ± 2	31 ± 9	1 ± 1	
	G-CSF		10 ± 4	0	0		
	M-CSF		1 ± 1	4 ± 2	35 ± 16		
	IL-3	4 ± 2	16 ± 7	10 ± 4	18 ± 4	1 ± 1	4 ± 2
	SCF	4 ± 2	17 ± 6	1 ± 1	0		
5.0 × 10^4 spleen cells/culture							
Asb-1$^{-/-}$ (n = 4)	GM-CSF		0.8 ± 1.0	0.3 ± 0.5	0.5 ± 1.0	0	
	IL-3	0.3 ± 0.5	0.8 ± 1.0	0.5 ± 1.0	1.0 ± 0.8	0	0.3 ± 0.5
C57BL/6 (n = 4)	GM-CSF		1.3 ± 2.5	0.5 ± 1.0	1.3 ± 2.5		
	IL-3	1.1 ± 0.6	1.0 ± 2.0	0.9 ± 1.4	0.9 ± 0.9	0	0.9 ± 0.9

[a] Cells were cultured in stimulus at a final concentration of 10 ng/ml (GM-CSF, G-CSF, M-CSF, and IL-3) or 100 ng/ml (SCF). Values are mean colony numbers ± standard deviations. G, granulocytic; GM, granulocyte-macrophage; M, macrophage; Eo, eosinophil; Meg, megakaryocyte.

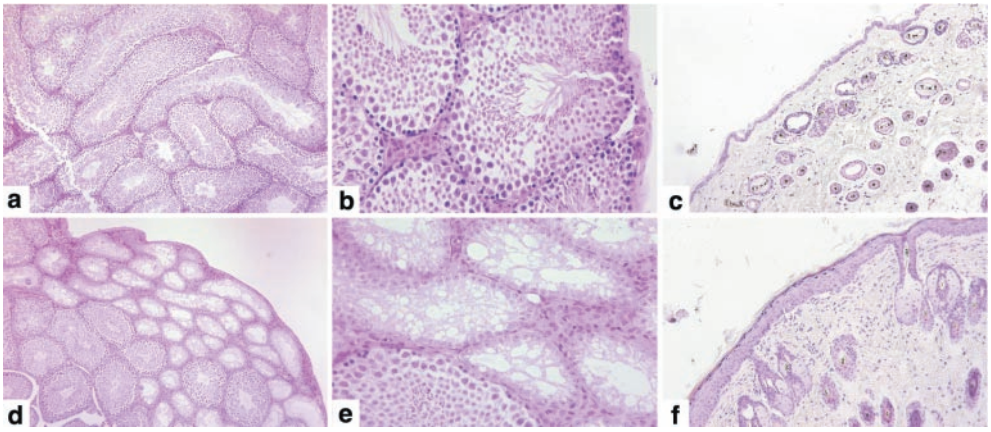

FIG. 3. Histology. The appearance of C57BL/6 testis (a and b) contrasts with that of Asb-1$^{-/-}$ testis (d and e), which shows a complete absence of spermatogenesis from some seminiferous tubules. Epithelial thickening is apparent in Asb-1$^{-/-}$ skin (f), contrasted with the appearance of normal C57BL/6 skin (c).

mates, 27 spleens from both Asb-1$^{-/-}$ and wild-type littermates were weighed, confirming a small, but statistically significant, lower weight of the spleen in Asb-1$^{-/-}$ mice (74.5 ± 9 mg versus 86.5 ± 14 mg; $P < 0.05$). However, histological examinations of Asb-1$^{-/-}$ spleens were normal, with splenic architecture and cellular composition apparently unperturbed. Thus, the mild reduction in spleen size in Asb-1$^{-/-}$ mice appears to reflect slightly reduced cellularity without significant loss of any particular cell subset.

Responses to various hematological stresses were examined by challenging Asb-1$^{-/-}$ mice with injections of phenylhydrazine, casein, or bacterial endotoxin (LPS). Mice injected with phenylhydrazine rapidly become anemic and subsequently respond with expanded erythropoiesis including increased production of BFU-E and CFU-E (17). In this experiment, hematocrit and numbers of BFU-E or CFU-E present in bone marrow or spleen were determined at 4 and 12 days after phenylhydrazine administration, representing peak response and recovery levels, respectively. No differences between knockout and control animals were observed (data not shown). The intraperitoneal injection of casein plus bacteria stimulates a rapid local accumulation of neutrophils from the bone marrow whose phagocytic activity clears the contaminating bacteria within 3 h (15). Three hours after the intraperitoneal administration of casein to eight Asb-1$^{-/-}$ mice and eight wild-type littermates, absolute neutrophil numbers in the peritoneal cavity and bone marrow revealed no differences between Asb-1$^{-/-}$ and control animals (data not shown). The pronounced elevation in hematopoietic progenitor cells normally observed following the injection of LPS (endotoxin) (19) also developed in LPS-injected Asb-1$^{-/-}$ mice. Changes in the numbers of hematopoietic cells in the spleen, bone marrow, peritoneum, and peripheral blood of the mice were also no different from controls when measured 6 days after LPS administration (data not shown).

Histopathology of Asb-1$^{-/-}$ mice. In sections of 18 organs from 2- to 3-month-old male and female Asb-1$^{-/-}$ mice, no morphological or pathological abnormalities were observed with the exception of changes in two organs.

In the testes of Asb-1$^{-/-}$ mice, there was frequently an overall appearance suggesting a diminution of spermatogenesis with less complete filling of seminiferous tubules. In accord with the known fertility of Asb-1$^{-/-}$ male mice, in no case were developing spermatozoa absent from the whole testis. In two blinded studies, using this criterion of relative emptiness of tubules, Asb-1$^{-/-}$ testes were correctly identified in 78 and 67% of cases, a frequency agreeing well enough with a frequency of 63% of underpopulated tubules recorded in an unblinded analysis. More striking was the occurrence of testes in which clusters of tubules entirely lacked developing spermatocytes (Fig. 3a to e). This appearance was seen in 31% of Asb-1$^{-/-}$ testes but in only 1 of 16 control C57BL/6 testes and 0 of 14 Asb-1 transgenic testes (Table 4). The anomolous testicular morphology had no apparent impact on the fertility

TABLE 4. Pathological changes in Asb-1$^{-/-}$ mice[a]

Parameter	C57BL/6		Asb-1$^{-/-}$		Asb-1 transgenic	
	Male	Female	Male	Female	Male	Female
Seminiferous tubules						
Depleted cellularity	2/16 (13)		10/16 (63)		1/14 (7)	
Empty tubules	1/16 (6)		5/16 (31)		0/14 (0)	
Skin epithelium						
Patchy thickening	1/14 (7)	0/8 (0)	4/16 (25)	0/10 (0)	3/14 (21)	0/9 (0)
Generalized thickening	1/14 (7)	0/8 (0)	5/16 (31)	0/10 (0)	4/14 (29)	0/9 (0)

[a] Values are shown as numbers of mice with characteristic/total numbers of mice (percentages of total).

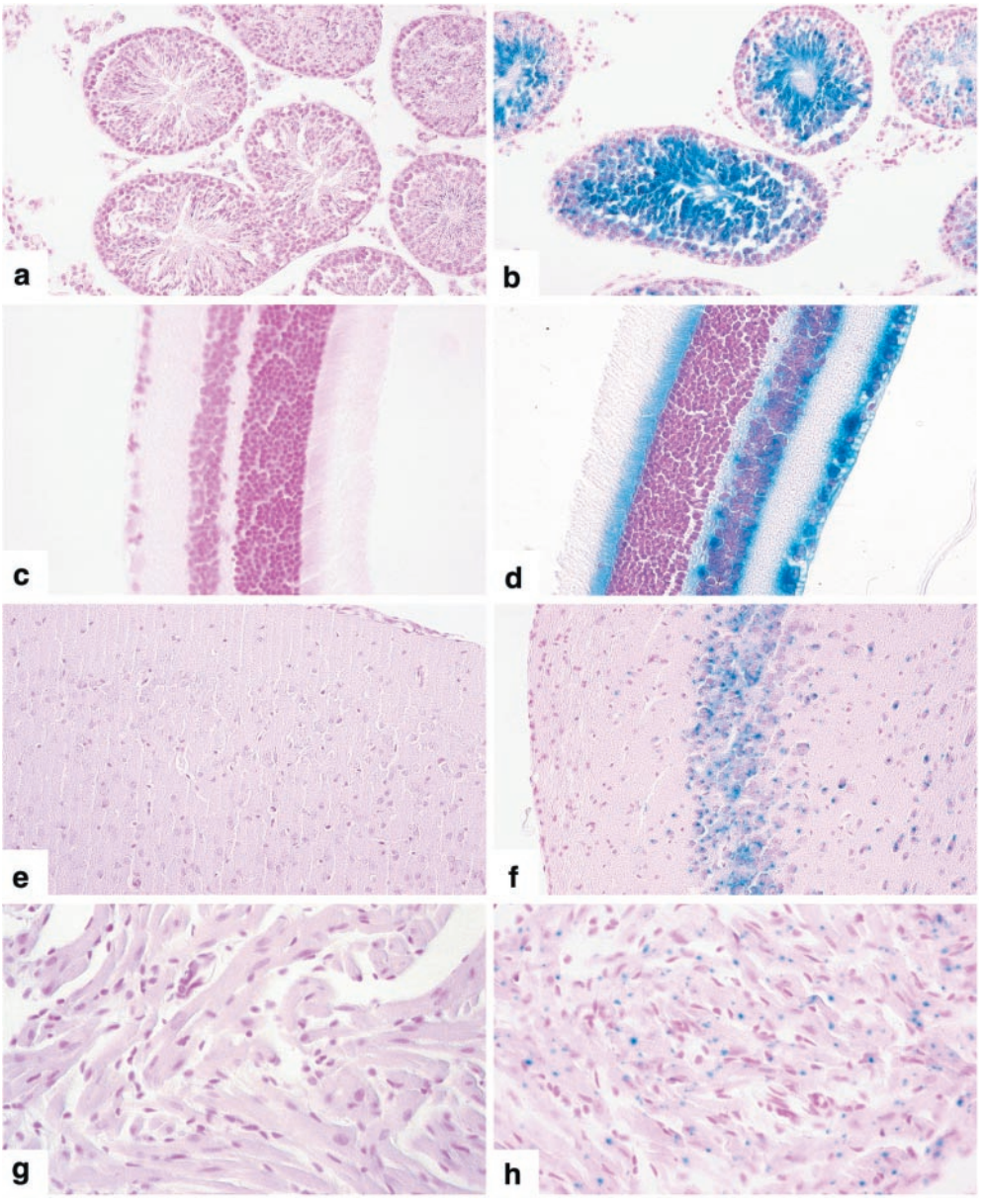

FIG. 4. LacZ staining of tissues from Asb-$1^{+/+}$ mouse testes (a), retina (c), cerebral cortex (e), and cardiac atrium (g) compared with that of Asb-$1^{-/-}$ testes (b), retina (d), cerebral cortex (f), and cardiac atrium (h).

of Asb-$1^{-/-}$ mice. We observed that each of six Asb-$1^{-/-}$ mice in our breeding program proved capable of siring litters. Eighteen litters from the six Asb-$1^{-/-}$ male mice averaged 6.7 ± 2 pups, and 18 litters from six Asb-$1^{+/-}$ male mice mated in parallel averaged 4.9 ± 2 pups.

A second abnormality observed in male mice was the occurrence of thickening of the epithelial layer of the skin, either in discrete patches or in a generalized distribution. This was associated with squamous differentiation and some keratin formation (Fig. 3f) but with no consistent infiltration of cells in the underlying dermis. This change was seen in 56% of Asb-$1^{-/-}$ male mice but only 14% of control C57BL/6 mice. The significance of this epithelial thickening is uncertain. It was also observed in 50% of male Asb-1 transgenic mice and has been observed in other groups of C57BL/6 mice under study in this laboratory at a higher frequency than seen in the formal group of C57BL/6 control males used in this study. Unrelated explanations such as scuffling or fighting cannot be excluded as the basis for the observed epithelial thickening.

LacZ staining of Asb-$1^{-/-}$ tissues. Homologous recombination between the targeting vector and the endogenous Asb-1 locus resulted in the in-frame fusion of the β-galactosidase gene with the 5′ coding region of exon 2, thereby placing β-galactosidase transcription under the control of the Asb-1 promoter region. To examine the pattern of β-galactosidase expression, adult mouse tissues were taken and fixed in 4% paraformaldehyde at 4°C for 1 h before staining overnight at 37°C in a 1-mg/ml X-Gal solution. Although this technique is subject to false-negative results due to inadequate diffusion of the substrate, the pattern of specific staining of Asb-$1^{-/-}$ tis-

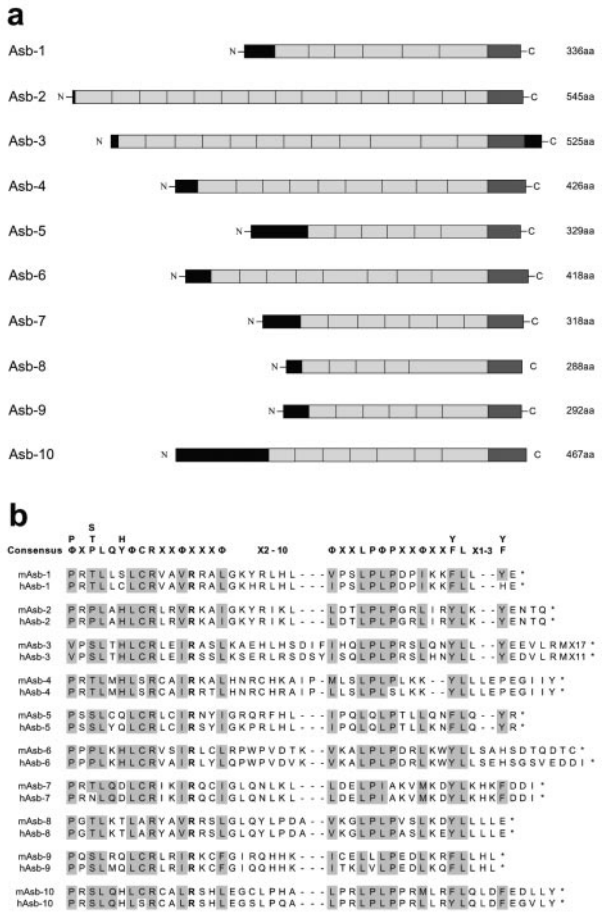

FIG. 5. (a) Predicted structures of the murine Asb family. Ankyrin repeats are shaded light grey, novel regions are black, and SOCS boxes are dark grey. aa, amino acids. (b) Alignment of the amino acid sequences of human and murine Asb SOCS boxes. Identities to the SOCS box consensus sequence (shown at top) are shaded grey. Terminating stop codons are indicated by an asterisk. The conserved arginine present in all Asb SOCS boxes identified to date is shown in boldface.

sues was striking and suggested that specific cell types in the mouse transcribe the Asb-1 gene. While the intensity of staining in tissues from Asb-$1^{+/-}$ mice was significantly decreased, the pattern was the same as that observed in tissues from Asb-$1^{-/-}$ mice. In the testes, developing and mature spermatocytes were strongly positive (Fig. 4b) but Sertoli cells were negative, as were many of the least mature spermatogonia. This pattern is of potential relevance in view of the defects in spermatogenesis noted in Asb-$1^{-/-}$ mice. Asb-1 transcription in the eye was also striking. Positive cells were the outermost lens epithelial cells, the inner layer (optic tract neurons) of the retina, and cells on both sides of the central bipolar retinal layer with a positive fringe of rod and cone processes projecting toward the eye capsule from the outer retinal layer (Fig. 4d). In parallel with this pattern, neurons were positive in a broad band in the cerebral cortex that did not extend to the meninges (Fig. 4f). Faint staining of doubtful significance was also observed in some groups of proximal tubule cells and collecting tubule cells in the kidney and in some hepatocytes. Cells of the cardiac atrium were consistently positive (Fig. 4h), and ventricular myocytes were stained less intensely. The positivity of bone marrow populations was noted above.

Expression of Asb family members in Asb-$1^{-/-}$ mice. In addition to the cloning of Asb-1 to Asb-4, continuing sequence database searches confirmed the existence of a further six members of the Asb family, all of which conform to the basic Asb structure of a central ankyrin repeat domain, a variable amino-terminal domain, and a carboxy-terminal SOCS box (GenBank accession numbers: Asb-5, AF398966; Asb-6, AF398967; Asb-7, AF398968; Asb-8, AF398969; Asb-9, AF398970; and Asb-10, AF398971). (Fig. 5a). A sequence alignment of the SOCS boxes from Asb-1 to Asb-10 is presented in Fig. 5b. While in most cases expressed sequence tags encoding new Asbs were identified, obtained, and sequenced, some protein sequences, particularly human ones, were predicted from sequence data present in databases. Of the new Asbs, Asb-10 is the largest, comprising 467 amino acids, while Asb-8 is the smallest, comprising 288 amino acids. Asb-10 possesses the largest amino-terminal region of any of the Asbs, a 110-amino-acid domain bearing no recognizable protein motifs or significant similarity to known proteins.

To determine whether Asb-$1^{-/-}$ mice show alterations in the expression patterns of other Asb family members, we conducted Northern blot analyses of poly(A)$^+$ RNA from a panel of Asb-$1^{-/-}$ and wild-type tissues. There were no gross changes in expression of mRNAs encoding Asb-2, Asb-3, Asb-4, Asb-5, Asb-6, Asb-8, Asb-9, and Asb-10 (Fig. 6).

Generation of Asb-1 transgenic mice. To complement our functional studies with knockout mice, two transgenes were constructed; both contained a human ubiquitin C promoter driving expression of either full-length or SOCS-box-deletion Asb-1 (Fig. 7a). In both cases, Asb-1 was Flag epitope tagged

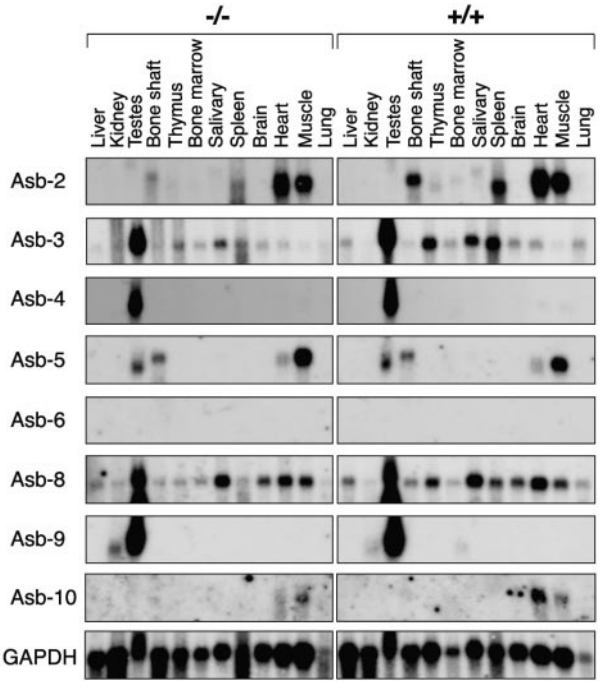

FIG. 6. Northern blot hybridization analysis of Asb mRNA expression in the tissues of Asb-1 knockout mice and wild-type littermates.

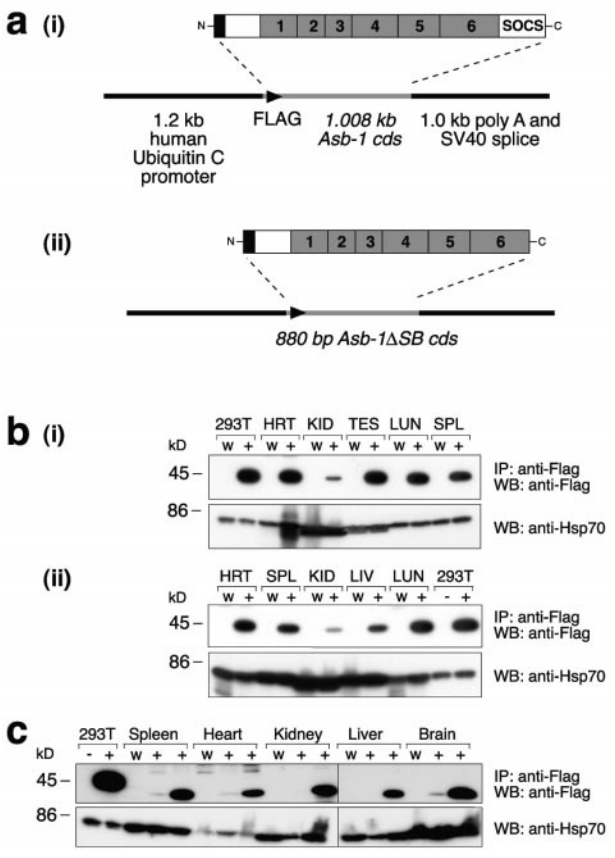

FIG. 7. (a) Schematic representation of the Asb-1 transgenes. The sequence encoding full-length (i) or SOCS-box-deletion Asb-1 (ii) was placed under the control of the human ubiquitin C promoter. (b) Immunodetection of full-length Asb-1 protein in the tissues of two lines (i and ii) of transgenic mice (+). HRT, heart; KID, kidney; TES, testes; LIV, liver; LUN, lung; SPL, spleen. 293T cells transfected with an Asb-1 expression vector (+) or vector alone (−) were included as a positive control. (c) Immunodetection of SOCS-box deletion Asb-1 protein in the tissues of two lines of transgenic mice. A significant difference in the level of Asb-1 protein expression between the two lines was observed. To control for loading, 2 μl of each lysate in panels b and c was Western blotted with rat anti-HSP70 antibody. SV40, simian virus 40; W, wild type; IP, immunoprecipitation; WB, Western blot.

to facilitate an examination of protein expression. Mice positive for the transgenes were identified at weaning, and colonies were established from two founders in each case. Northern blot hybridization analysis showed that both transgenes were expressed at levels 5- to 10-fold above endogenous Asb-1 levels (data not shown). Immunoprecipitations and Western blotting with anti-Flag antibodies detected proteins of the expected sizes in transgenic but not wild-type tissues. Two lines positive for the full-length Asb-1 transgene appeared to express similar levels of the Flag-tagged Asb-1 protein, which migrated with an apparent molecular mass of 39 kDa (Fig. 7b), while the two lines carrying the truncated Asb-1 transgene showed a 10- to 20-fold difference in expression of the SOCS-box-deletion Asb-1 protein with a slightly lower apparent molecular mass of 35 kDa. Both full-length and SOCS-box-deletion Asb-1 transgenic animals were healthy and fertile. They showed no gross histological abnormalities, organ weight disparities, or hematopoietic perturbations in the range of assays outlined above, with the exception of male transgenic mice expressing SOCS-box-deletion Asb-1, which showed an approximately 25% decrease in the weight of both testes and salivary gland ($P < 0.005$). Histological sections of these organs, however, revealed no abnormalities that might explain such a difference.

DISCUSSION

Ankyrin repeats have been identified in more than 400 proteins in eukaryotes, bacteria, and viruses (4). The archetypal ankyrin repeat of 33 amino acids forms a V-shaped β-hairpin–α-helix–turn–α-helix–loop motif, with consecutive repeats stacking sequentially in bundles (6). It is clear that ankyrin repeats are a generic structural motif involved in protein-protein interactions, and as such, their presence provides little insight into the function of a novel protein. The SOCS box motif is thought to act as an adaptor via which SOCS box-containing proteins, and/or their protein partners, are targeted for proteasomal degradation (8, 23). Thus, given the exquisite specificity of ankyrin repeats, it is tempting to speculate that the Asbs act to target a class or classes of interacting partner proteins for degradation. In an attempt to understand what cellular processes might be regulated by the Asbs, we have generated mice deficient for Asb-1. This deficiency had no obvious deleterious effects on normal development, with the possible exception of a subtle defect in testicular cellularity. Hemopoiesis in Asb-1$^{-/-}$ mice, both at steady state and in response to several forms of hematopoietic stress, appeared normal, despite expression of Asb-1 in wild-type hematopoietic cells.

Given that Asb-1 is one of a 10-member family of ankyrin repeat SOCS box-containing proteins, the lack of an overt phenotype in Asb-1$^{-/-}$ mice raises the possibility of overlapping or shared functions between individual members of the family. In this context, it is interesting to note that some overlap does exist in the mRNA expression patterns of the Asbs in normal mouse tissues. Asb-2, Asb-5, and Asb-10 share similar expression patterns, their mRNAs most prominently seen in heart and muscle. Asb-1 and Asb-3 are both widely expressed, their mRNAs detected in all tissues examined. It is therefore possible that Asb-1 deficiency in experimental animals is compensated for by the actions of another Asb. This may or may not require the upregulation of mRNA expression of the latter. Northern blot hybridization analysis of Asb mRNA expression in the tissues of Asb-1$^{-/-}$ mice and wild-type littermates revealed no gross changes in the expression of Asb-2, Asb-3, Asb-4, Asb-5, Asb-6, Asb-8, Asb-9, or Asb-10. However, functional redundancy may still operate via normal expression levels. A more detailed examination of Asb expression at the cellular level, in combination with an analysis of mice lacking multiple Asbs, may begin to directly address this issue.

The fact that overexpression of full-length Asb-1 has no apparent effect on transgenic animals may further suggest that Asb-1 is a protein whose level of expression is not critical. However, if Asb-1 is indeed targeting partner proteins for degradation via the SOCS box, a possibility supported by work demonstrating that the SOCS box of Asb-2 can bind the elongin BC complex (8, 23), one might expect the overexpression of SOCS box-deletion Asb-1 to have a dominant negative effect. Although this appears not to be the case in the mice studied

here, a more complete understanding of the biochemical role of the SOCS box within the Asb family will be required to fully interpret our observations in genetically modified mice.

ACKNOWLEDGMENTS

We are grateful to Peter Angel, Deutsches Krebsforschungszentrum, Heidelberg, Germany, for the gift of the UBI-*junB* plasmid. We thank Kathy Hanzinikolas for expert animal husbandry and Janelle Mighall for excellent technical assistance.

This work was supported by the National Health and Medical Research Council, Canberra; the Anti-Cancer Council of Victoria; an Australian Government Cooperative Research Centres Program grant; the National Institutes of Health, Bethesda, grant CA22556; the J. D. and L. Harris Trust; and AMRAD Operations Pty. Ltd., Melbourne. B.T.K. is the recipient of an Australian Postgraduate Award.

REFERENCES

1. **Alexander, W. S., D. Metcalf, and A. R. Dunn.** 1995. Point mutations within a dimer interface homology domain of c-Mpl induce constitutive receptor activity and tumorigenicity. EMBO J. **14:**5569–5578.
2. **Alexander, W. S., A. W. Roberts, N. A. Nicola, R. Li, and D. Metcalf.** 1996. Deficiencies in progenitor cells of multiple hematopoietic lineages and defective megakaryocytopoiesis in mice lacking the thrombopoietic receptor c-Mpl. Blood **87:**2162–2170.
3. **Alexander, W. S., R. Starr, J. E. Fenner, C. L. Scott, E. Handman, N. S. Sprigg, J. E. Corbin, A. L. Cornish, R. Darwiche, C. M. Owczarek, T. W. Kay, N. A. Nicola, P. J. Hertzog, D. Metcalf, and D. J. Hilton.** 1999. SOCS1 is a critical inhibitor of interferon gamma signaling and prevents the potentially fatal neonatal actions of this cytokine. Cell **98:**597–608.
4. **Bork, P.** 1993. Hundreds of ankyrin-like repeats in functionally diverse proteins: mobile modules that cross phyla horizontally? Proteins **17:**363–374.
5. **Elefanty, A. G., C. G. Begley, D. Metcalf, L. Barnett, F. Kontgen, and L. Robb.** 1998. Characterization of hematopoietic progenitor cells that express the transcription factor SCL, using a lacZ "knock-in" strategy. Proc. Natl. Acad. Sci. USA **95:**11897–11902.
6. **Gorina, S., and N. P. Pavletich.** 1996. Structure of the p53 tumor suppressor bound to the ankyrin and SH3 domains of 53BP2. Science **274:**1001–1005.
7. **Hilton, D. J., R. T. Richardson, W. S. Alexander, E. M. Viney, T. A. Willson, N. S. Sprigg, R. Starr, S. E. Nicholson, D. Metcalf, and N. A. Nicola.** 1998. Twenty proteins containing a C-terminal SOCS box form five structural classes. Proc. Natl. Acad. Sci. USA **95:**114–119.
8. **Kamura, T., S. Sato, D. Haque, L. Liu, W. G. Kaelin, Jr., R. C. Conaway, and J. W. Conaway.** 1998. The elongin BC complex interacts with the conserved SOCS-box motif present in members of the SOCS, ras, WD-40 repeat, and ankyrin repeat families. Genes Dev. **12:**3872–3881.
9. **Kile, B. T., W. S. Alexander, and N. A. Nicola.** 2001. Negative regulators of cytokine signaling. Int. J. Hematol. **73:**292–298.
10. **Kile, B. T., E. M. Viney, T. A. Willson, T. C. Brodnicki, M. R. Cancilla, A. S. Herlihy, B. A. Croker, M. Baca, N. A. Nicola, D. J. Hilton, and W. S. Alexander.** 2000. Cloning and characterisation of the genes encoding the ankyrin repeat and SOCS box-containing proteins Asb-1, Asb-2, Asb-3 and Asb-4. Gene **258:**31–41.
11. **Kimura, S., A. W. Roberts, D. Metcalf, and W. S. Alexander.** 1998. Hematopoietic stem cell deficiencies in mice lacking c-Mpl, the receptor for thrombopoietin. Proc. Natl. Acad. Sci. USA **95:**1195–1200.
12. **Marine, J. C., C. McKay, D. Wang, D. J. Topham, E. Parganas, H. Nakajima, H. Pendeville, H. Yasukawa, A. Sasaki, A. Yoshimura, and J. N. Ihle.** 1999. SOCS3 is essential in the regulation of fetal liver erythropoiesis. Cell **98:**617–627.
13. **Marine, J. C., D. J. Topham, C. McKay, D. Wang, E. Parganas, D. Stravopodis, A. Yoshimura, and J. N. Ihle.** 1999. SOCS1 deficiency causes a lymphocyte-dependent perinatal lethality. Cell **98:**609–616.
14. **Metcalf, D., C. J. Greenhalgh, E. Viney, T. A. Willson, R. Starr, N. A. Nicola, D. J. Hilton, and W. S. Alexander.** 2000. Gigantism in mice lacking suppressor of cytokine signalling-2. Nature **405:**1069–1073.
15. **Metcalf, D., L. Robb, A. R. Dunn, S. Mifsud, and L. Di Rago.** 1996. Role of granulocyte-macrophage colony-stimulating factor and granulocyte colony-stimulating factor in the development of an acute neutrophil inflammatory response in mice. Blood **88:**3755–3764.
16. **Nicholson, S. E., U. Novak, S. F. Ziegler, and J. E. Layton.** 1995. Distinct regions of the granulocyte colony-stimulating factor receptor are required for tyrosine phosphorylation of the signaling molecules JAK2, Stat3, and p42, p44MAPK. Blood **86:**3698–3704.
17. **Rickard, K. A., N. J. Rencricca, R. K. Shadduck, F. C. Monette, D. E. Howard, M. Garrity, and F. Stohlmann.** 1971. Myeloid stem cell kinetics during erythropoietic stress. Br. J. Haematol. **20:**537–547.
18. **Schorpp, M., R. Jager, K. Schellander, J. Schenkel, E. F. Wagner, H. Weiher, and P. Angel.** 1996. The human ubiquitin C promoter directs high ubiquitous expression of transgenes in mice. Nucleic Acids Res. **24:**1787–1788.
19. **Staber, F. G., and D. Metcalf.** 1980. Cellular and molecular basis of the increased splenic hemopoiesis in mice treated with bacterial cell wall components. Proc. Natl. Acad. Sci. USA **77:**4322–4325.
20. **Starr, R., D. Metcalf, A. G. Elefanty, M. Brysha, T. A. Willson, N. A. Nicola, D. J. Hilton, and W. S. Alexander.** 1998. Liver degeneration and lymphoid deficiencies in mice lacking suppressor of cytokine signaling-1. Proc. Natl. Acad. Sci. USA **95:**14395–14399.
21. **Starr, R., T. A. Willson, E. M. Viney, L. J. Murray, J. R. Rayner, B. J. Jenkins, T. J. Gonda, W. S. Alexander, D. Metcalf, N. A. Nicola, and D. J. Hilton.** 1997. A family of cytokine-inducible inhibitors of signalling. Nature **387:**917–921.
22. **Strasser, A., A. W. Harris, and S. Cory.** 1991. bcl-2 transgene inhibits T cell death and perturbs thymic self-censorship. Cell **67:**889–899.
23. **Zhang, J. G., A. Farley, S. E. Nicholson, T. A. Willson, L. M. Zugaro, R. J. Simpson, R. L. Moritz, D. Cary, R. Richardson, G. Hausmann, B. T. Kile, S. B. Kent, W. S. Alexander, D. Metcalf, D. J. Hilton, N. A. Nicola, and M. Baca.** 1999. The conserved SOCS box motif in suppressors of cytokine signaling binds to elongins B and C and may couple bound proteins to proteasomal degradation. Proc. Natl. Acad. Sci. USA **96:**2071–2076.